Ultrasound in Med. & Biol., Vol. 28, No. 1, pp. 49–57, 2002

0301-5629/02/$–see front matter

PII: S0301-5629(01)00486-0

● *Original Contribution*

POWER M-MODE DOPPLER (PMD) FOR OBSERVING CEREBRAL BLOOD FLOW AND TRACKING EMBOLI

MARK A. MOEHRING* and MERRILL P. SPENCER†
*Spencer Technologies, Seattle, WA, USA and †Spencer Vascular Laboratories, Seattle, WA, USA

(*Received* 13 *July* 2001; *in final form* 3 *October* 2001)

Abstract—Difficulties in location of transcranial ultrasound (US) windows and blood flow in cerebral vessels, and unambiguous detection of microemboli, have limited expansion of transcranial Doppler US. We developed a new transcranial Doppler modality, power M-mode Doppler (PMD), for addressing these issues. A 2-MHz digital Doppler (Spencer Technologies TCD100M) having 33 sample gates placed with 2-mm spacing was configured to display Doppler signal power, colored red and blue for directionality, in an M-mode format. The spectrogram from a user-selected depth was displayed simultaneously. This system was then explored on healthy subjects and patients presenting with varying cerebrovascular pathology. PMD facilitated window location and alignment of the US beam to view blood flow from multiple vessels simultaneously, without sound or spectral clues. Microemboli appeared as characteristic sloping high-power tracks in the PMD image. Power M-mode Doppler is a new paradigm facilitating vessel location, diagnosis, monitoring and microembolus detection. (E-mail: mm@spencertechnologies.com) **© 2002 World Federation for Ultrasound in Medicine & Biology.**

Key Words: **Transcranial Doppler, M-mode, Embolism, Ultrasound, Microemboli.**

INTRODUCTION

Since the advent of transcranial Doppler (TCD), its acceptance has been impeded by the difficulties in finding temporal bone and other ultrasonic windows through the skull. In elderly populations, where the technology is greatly needed, 10% to 15% of individuals have no transtemporal window. Frustrating time is consumed in finding the available windows in many patients. Even the pathways through the natural windows of the orbit and foramen magnum are often difficult to use because of the need to explore each depth one step at a time with single-gate TCD equipment. New approaches are needed to ease the task of window assessment and flow location.

New approaches are also needed for detecting and counting cerebral microemboli. A decade has passed since initial transcranial observations of microemboli in the cerebral circulation using single-gate pulsed Doppler ultrasound (US) (Padayachee et al. 1987; Spencer et al. 1990). Detection of cerebral microemboli has been used to explore pathologies from which microemboli arise in the heart and peripheral vessels, and has helped reduce the incidence of stroke during surgery of the carotid artery (Spencer 1997; Ackerstaff et al. 2000). Identification of microembolic signals and discrimination from artefacts (high-intensity transient signals of nonembolic origin) with single-gate TCD equipment, nevertheless, remains a complex challenge to both human and machine observers (Ringlestein et al. 1998; Cullinane et al. 2000).

The single-gate spectrogram recommends itself for detecting microemboli by being the most convenient tool at hand, being well-established and widespread in use for evaluating cardiac and peripheral vascular hemodynamics. Observation of an embolic signal in a single-gate spectrogram is, by definition, however, partial evidence—a fleeting glimpse—of a microembolus. The definition of an embolus stipulates movement from one place to another in the bloodstream. The single-gate spectrogram observes velocity and US echo amplitude at one place. An argument might be made that the sample volume for the single-gate Doppler is, indeed, a volume of space and, therefore, contains more than one depth, but this volume covers a small fraction of the migration path of an embolus.

Embolic behavior on the typical spectrogram is often a challenge to confirm because the time-duration of the embolic presence in the spectrogram is often of similar order to the analysis period for one spectral line, typically ~10 ms. The fast Fourier transform (FFT) by

Address correspondence to: Mark Moehring, PhD, Spencer Technologies, 701 16th Avenue, Seattle, WA 98122 USA. E-mail: mm@spencertechnologies.com

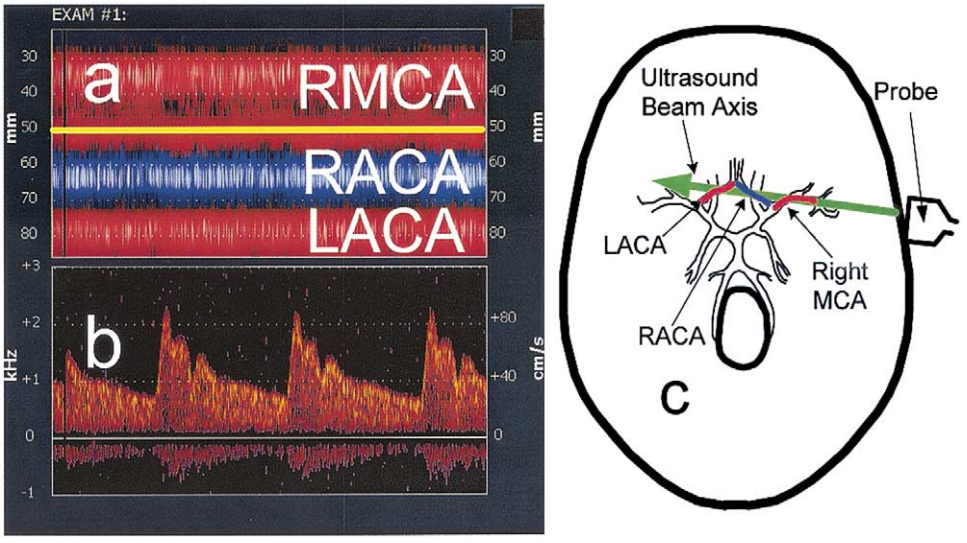

Fig. 1. Example power M-mode Doppler (PMD) observation of cerebral blood flow. (a) Demonstration of beam alignment with the right middle cerebral artery (RMCA), the right anterior cerebral artery (RACA), and the left anterior cerebral artery (LACA). (b) Concurrent spectrogram from 50-mm gate depth (MCA). (c) Schematic of beam intersection with intracranial vessels shown in PMD image.

nature will spectrally broaden a microembolic signal in the spectrogram, if the microembolus does not travel at a constant velocity for the entire analysis period for one spectral line. Dynamic range limitations of current analog TCD systems lead, as well, to extraspectral embolic signatures. These factors lie behind the ambiguity between embolic signatures and artefacts observed in the spectrogram.

Doppler systems having multiple spectrograms associated with different depth locations have been explored for watching the progress of an embolus over depth (Spencer 1992; Nabavi et al. 1996). Observation of the raw time series Doppler shift signatures from multiple depths has also been employed for observing embolus movement. These methods place multiple images on the display, and the user can then interpret whether a signature arises from an embolus or an artefact by its progress from depth to depth. This process increases the complexity of detecting emboli because of the need to evaluate multiple images for each potential embolic signal, especially for the observer who does not have expertise in US.

The work reported here presents a basic change in how pulse Doppler information is processed, to the end of creating a new display from which locating transcranial windows is facilitated, blood flow in desired arteries is quickly selected and microemboli are uniquely identified and intuitively discriminated from artefacts. This new display is customized to the definition of a microembolus, in that an image of blood flow across time and depth is captured and, in this format, an embolus can be observed transiting along a blood vessel. The system that produces this new image modality is described below, and diagnostic transcranial blood flow signals, microemboli and artefact observations are presented to illustrate its utility.

MATERIALS AND METHODS

Transcranial Doppler studies for this work were performed with the TCD100M (Spencer Technologies, Seattle, WA) which calculates a power M-mode Doppler (PMD) image concurrently with a single-gate spectrogram. An example image of the presentation format for this modality is shown in Fig. 1. The PMD image in Fig. 1a resides above the spectrogram image of Fig. 1b, so that they share the same horizontal time axis. The PMD image shows depth from the probe on the vertical axis, time on the horizontal axis, and power of the Doppler shift signal at specific depths as color intensity. Simultaneously, the direction of blood flow is derived from the positive or negative mean value of the Doppler shift signal at the particular depth. This mean velocity information is used in the PMD image as red, depicting flow toward the probe and blue, as flow away from the probe. As each new line in the spectrogram is calculated and displayed, a corresponding PMD line is displayed concurrently in the PMD image directly above. The horizontal yellow line in the PMD display in Fig. 1a indicates the gate depth associated with the spectrogram in Fig. 1b. In Fig. 1a, bands of color running horizontally across the image

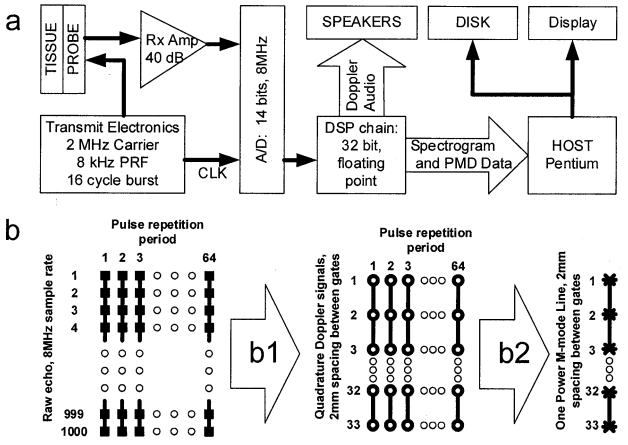

Fig. 2. (a) System diagram of TCD100M, which processes PMD, spectrogram and audio output concurrently. (b) Blowup of digital signal processing (DSP) stage of Fig. 2a. Initial data consisted of 1000 digitized values (■) for each of 64 PRPs. Two major processing steps were then accomplished: (b1) low-pass filtering and decimation was performed to obtain (○) quadrature Doppler samples at 33 different gate depths and for each of 64 PRPs, and (b2) combination of first and zeroth lag autocorrelation values at each depth to obtain (*) 33 directional power M-mode samples.

indicate the location of blood flow along the beam axis. A schematic of the anatomy from which the PMD image is derived is drawn in Fig. 1c.

The method exemplified in Fig. 1 is different from color velocity imaging techniques developed previously (Eyer et al. 1981; Omoto R. et al. 1984), in that PMD displays changes in signal power from moving targets as change in color intensity; higher power is displayed as lighter color (*i.e.*, dark red for low power to pink for high power). Changes in velocity do not affect change in intensity of color of the PMD image. In the PMD display, emboli will appear as high-power transient signatures or light-colored "tracks" (Moehring 2000). Emboli in traditional color velocity image format will be invisible because their velocity does not distinguish them from that of surrounding blood flow.

Power M-mode image construction

Figure 2a illustrates the system that simultaneously produces the spectrogram and PMD displays of Fig. 1. The transmit burst throughout this work consists of 16 cycles at 2 MHz launched from a 13-mm diameter circular transducer, making an effective sample volume axial length of 6 mm. The TCD100M accomplishes power M-mode image construction, as further illustrated in Fig. 2b, by first digitizing received US echoes immediately after amplification and then fully processing all Doppler information digitally. This device accomplishes bilateral image construction by utilizing most of its capacity for over 300 million math operations per s, utilizing eight high-speed digital signal processing chips (1 TMS320c549 processor and 3 TMS320c31 processors on each Doppler channel). The example given here is for the case of 8-kHz pulse-repetition frequency (PRF). The TCD100M system processes 125 lines per s for display, or 8 ms per line. During each 8-ms period, a total of 64,000 US echo samples are gathered. These 64,000 samples are spread uniformly across 64 pulse repetition periods (PRPs) of the Doppler (that is, 1000 samples are acquired from each PRP). The digital sampling of the US echo throughout this work is done at 4 times the 2-MHz carrier frequency, or 8 MHz, and at 14 bits (84 dB) dynamic range. The usable dynamic range above the noise background for this digital Doppler system measures minimally at 78 dB at the point of digitization, and filtering operations in the digital environment further enhance the signal-to-noise ratio (SNR) by 10 to 20 dB.

Digitization of US echoes during each pulse period at 4 times the carrier frequency enables the construction of one Doppler shift signal sample using each successive group of four digitized values. In each nonoverlapping group of four samples, the real value of the baseband Doppler shift signal is obtained from the difference of the first and third sample, and the imaginary value of the baseband Doppler shift signal is obtained from the subtraction of the second and fourth values. A total of 1000 US echo samples from one pulse period are, thus, transformed into 250 Doppler shift samples from 250 evenly spaced gate depths. The spacing between adjacent gate depths is half a wavelength of the carrier frequency, or $\sim$385 μ. This set of Doppler shift values for one pulse period is low-pass filtered to reject noise outside the frequency bandwidth of the transmit burst, and resampled to obtain one sample gate every 2 mm in depth. The PMD images reported here display a range in depth from 24 to 88 mm with a sample spacing of 2 mm and are, thus, constructed from a total of 33 sample gates. Deeper ranges of the PMD image vertical depth scale, as shown in some of the images below, are obtained using lower PRFs than 8 kHz.

The spectrogram and the associated stereo audio output of the system are obtained from an additional 34th sample gate. The depth location of this last gate is under user control and can be positioned arbitrarily in 1-mm increments. The spectral display is calculated with a 128-point FFT, 50% overlap at 8 kHz PRF and with a Hanning window. The PMD calculations utilize no data windows and have no overlap with adjacent 8-ms calculation periods. (For the PMD image line, a window is not required as in the spectrogram FFT because the PMD image is not constructed from a transform sensitive to endpoint discontinuities in the data.) Both the PMD and

spectral displays are log compressed so that a particular range of color on the output display is proportional to a user-selected range of dB of the input signal.

Signal autocorrelation is used to calculate, respectively, the power (0th lag) and the average Doppler shift frequency (1st lag) (Kasai et al. 1985) at each gate depth. The color and intensity assigned to each gate is done as a function of power and independent of velocity, with one exception: **velocities** close to zero (below the clutter cancellation frequency of 200 Hz or 7 cm/s) are assigned no color (black) in the PMD image. This has important implications in turbulence and microembolus detection, discussed below. **Power** below a user-controlled level is also assigned no color (black). Thus, the user can set a threshold above which nominal signals are given color and below which noise is colored black.

Results reported below reflect exploration of this device in the vascular lab and surgical setting over a 3-year time frame. Provision was made to record a continuous stream of data to hard disk for a minimum of 10-h at a time, or save 8-s snapshots of data of interest. Recorded data are replayable by reprocessing the digitized data stored to disk and can, as well, be exported to an external computer for constructing the images shown in this report.

RESULTS

Location of transcranial windows and blood flow

Application of PMD with the TCD100M showed that the US probe can be aimed through the temporal bone so that multiple vessels simultaneously appear in the PMD image. Figure 1a demonstrates that the ipsilateral MCA and ACA, as well as the contralateral ACA, can be aligned within the same beam path with PMD. Figure 1b shows the concurrent normal right middle cerebral artery (RMCA) spectrogram obtained with a single gate placed at a depth of 50 mm.

Displaying color as a function of signal power at multiple depths offers advantages for an examiner to locate a temporal bone window without limiting interrogation to a single selected depth. When employed in assessment of patients at various vascular laboratories, the sonographers reported that PMD TCD was easier to use because it was no longer necessary to seek a window by changing depth. Also, they found it unnecessary to listen for a Doppler sound. In fact, PMD enabled them to first find the optimal temporal window on the PMD display and then to adjust the gate depth for audible spectral display using the PMD depth scale. PMD allowed the examiner to find the temporal window without audible Doppler sounds and, therefore, avoid crashing sounds of probe application to the head. During intraoperative monitoring, the sonographers maintained their position on the window using the color signals present in the PMD image as a guide. When the flow signals were accidentally lost during surgical monitoring, these could be recovered by repositioning the transducer using the PMD display only. Therefore, the significant problem of single-gate TCD (*i.e.,* frustration in locating difficult windows) was reduced.

Transcranial examinations through the orbit and foramen magnum were performed by identifying the vessel of interest according to depth and direction of blood flow. For example, Fig. 3 illustrates the transorbital PMD and spectral findings in a patient with severe stenosis of the left internal carotid artery. Output power was reduced to 10% (< 70 mW/cm^2 spatial peak temporal average intensity) in this case. Panel A of Fig. 3 demonstrates a reversed flow with high velocities in the left ophthalmic artery seen on the PMD display at a depth of 40 mm behind the eyelid. This high-velocity flow represents collateral flow to the distal left ICA and MCA. The panel on the right demonstrates normally directed flow in the right ophthalmic artery seen on the PMD display at a depth of 48 mm.

Figure 4 illustrates the transforaminal PMD and spectral findings in a patient in whom a stenosis of the left subclavian artery was found. Figure 4a demonstrates the left vertebral artery spectrum found through the foramen magnum at a depth of 70 mm and showing a bimodal systolic acceleration typical of early proximal obstruction. Figure 4b shows a normal spectrum of the basilar artery found at a depth of 104 mm through the foramen magnum of the same patient. The normal basilar waveform and velocity demonstrate the sufficiency of supply from the right vertebral artery.

Turbulence and bruits, as well as aliased blood flow velocities, can appear on PMD with distinguishing characteristics. Figure 5 shows a case of severe MCA vasospasm after subarachnoid hemorrhage, demonstrating bruits and high velocities at the depth range of 35 to 45 mm. The dark regions at the 41-mm sample gate depth indicate sample gates at which the mean velocity detected by Doppler is less than the clutter filter cutoff of 7 cm/s. Note that this corresponds to bruit appearance on the spectrogram below. The spectrogram display intensity is on a logarithmic scale, and the bright low-velocity regions near 0 and 8-kHz severely bias the mean velocities and result in the associated dark reigons in the PMD image. The places of lighter color, just outside the black regions at the 41-mm sample gate depth in the PMD image, are where the bruit was not strong enough to drive the mean velocity close to zero. The spectrogram also shows high velocity aliasing that accentuates during systole, and shows on PMD as bits of blue speckle in the vicinity of the spectrogram sample volume. These characteristic signatures of aliasing and turbulence in the

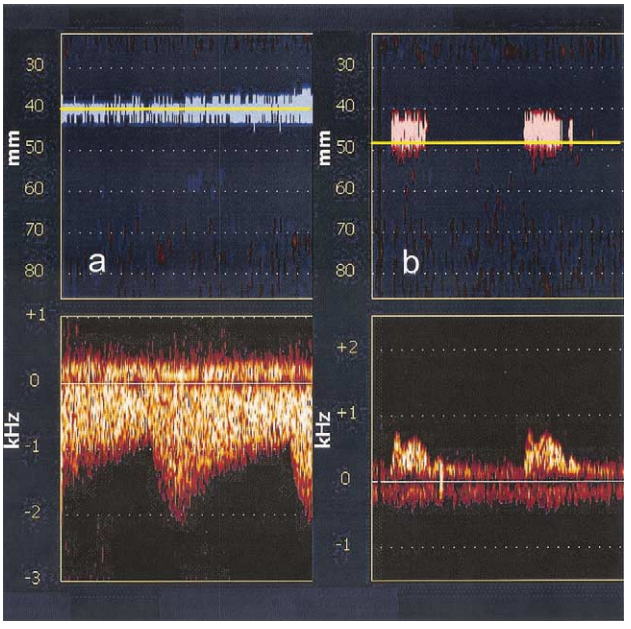

Fig. 3. Transorbital PMD and spectrogram findings in a patient with severe left ICA stenosis. (a) Reversed flow with high velocities in the left ophthalmic artery. (b) Normal direction flow in the right ophthalmic artery seen on the PMD display.

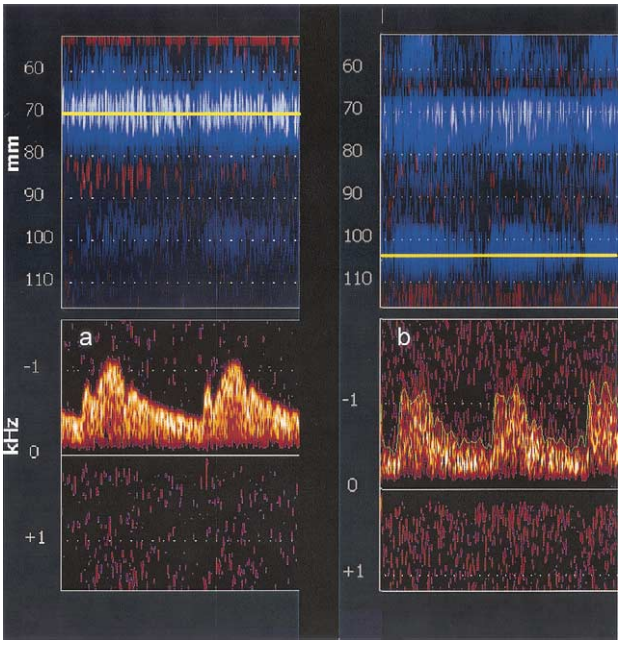

Fig. 4. Use of a deeper depth range in transforaminal PMD and spectral findings in a patient with stenosis of the left subclavian artery and in which the PMD image served as a guide for quick location of the desired flow: (a) left vertebral artery and (b) basilar artery at depth of 104 mm through the foramen magnum.

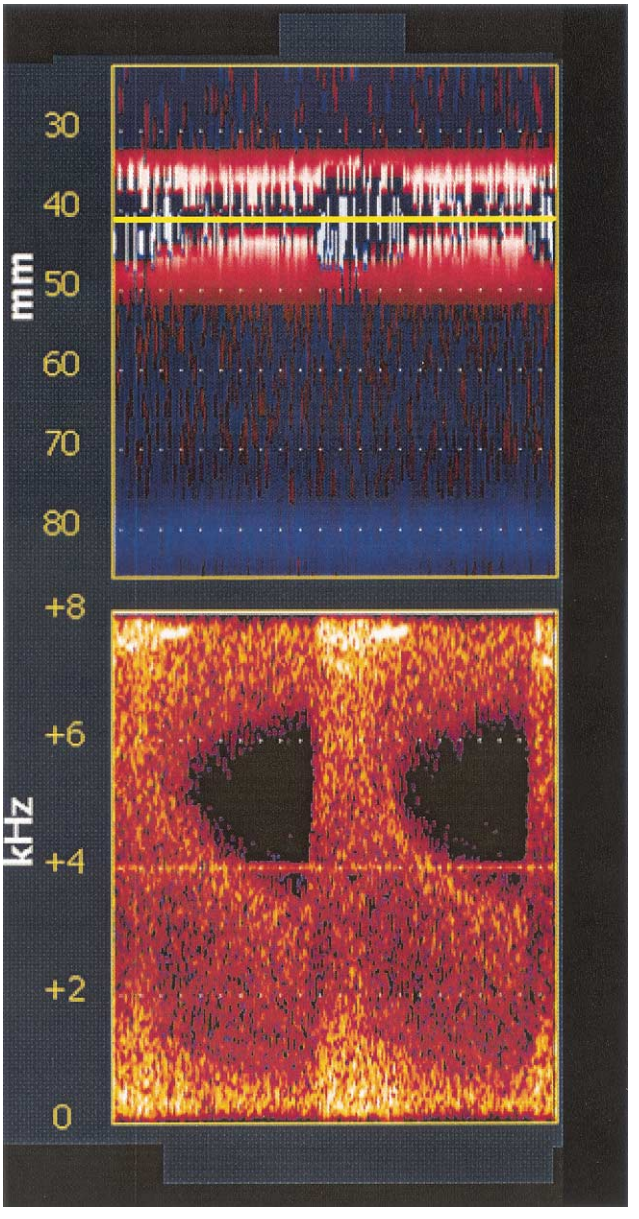

Fig. 5. Severe turbulence manifestation on the PMD display in a patient with MCA vasospasm. Note that mean velocities less than the clutter cutoff of 7 cm/s appear as black in the PMD display and are most pronounced during systole. The 4 kHz tone in the spectrogram is an early prototype artefact.

PMD image were particularly useful in finding the associated stenotic regions at very shallow depth range of insonation. This abnormal PMD pattern can be first visualized and then used to guide sample volume exploration of the spectral characteristics of the associated blood flow. The depth of this signal is in the distal MCA, a region that is often overlooked by examiners using single-gate Doppler.

The high-intensity color in the PMD image of Fig.

5, which is associated with turbulence, is in the vicinity of 20 dB above the flow signals at the edge of the MCA region under study. There are similar, although not as dramatic, high-intensity colors in the RACA blue region of Fig. 1 that are not associated with turbulence in this vessel. The system gain in the latter case has been set so that the RACA signal is mapped into the brighter region of the "map" that transforms power to color. This is a user-controllable function in the TCD100M and can be adjusted by the user to maintain normal blood flow in a nonsaturating color region. This effectively grooms the system for observing abnormally high power as turbulence or emboli, and can be adjusted during playback of recorded data.

Microembolic "tracks"

A volunteer subject with a mechanical mitral valve and aortic composite valve graft (St. Jude, Minneapolis, MN) was observed at multiple sessions to gain experience in PMD observation of embolic signals. During each session, the subject was fitted with a probe fixation head frame (Marc Series, Spencer Technologies, Seattle, WA), and the probe was held in a fixed position for the entire session. Several hundred microembolic tracks, as identified by the authors, were collected using the TCD100M system. The gate associated with the spectrogram was placed at a variety of depths. During these sessions, two vessels were typically in view on PMD. Multiple microembolic signals were recorded during these sessions and representative images are shown to illustrate the varied appearances of microembolic tracks and artefact signals using PMD imaging.

Two microemboli in different vessels are shown in Fig. 6, and appear as high-power tracks in the PMD image. Blood flow in this figure is from the middle cerebral artery (MCA, red) and anterior cerebral artery (ACA, blue). The spectrogram is acquired at 40 mm depth in Fig. 6a (MCA), and at 67 mm depth in Fig. 6b (ACA). These embolic tracks in the MCA and the ACA PMD images have simultaneous spectrogram signatures. The spectrogram signatures are restricted to the point in time that the PMD embolic track crosses the gate depth associated with the spectrogram (yellow line). Both embolic tracks of Fig. 6 have slopes consistent with their movement direction. The MCA microembolus, which moves toward the probe as time progresses, has a positive sloped track within the image. The ACA microembolus, which moves away from the probe as time progresses, has a negative sloped track within the image. Microemboli appear in the spectrogram as high-power/high-intensity transient unidirectional signals. Their spectrogram appearance corresponds to the definition of a microembolic signature forged by the Consensus committee of the 9th Cerebrovascular Hemodynamics Symposium (Ackerstaff et al. 1995).

PMD embolic tracks can display complex behavior. In Fig. 7a, for example, an embolus is shown in transit in the PMD image from a depth of 67 mm to a depth of about 45 mm, then reappears and resumes its course into the distal MCA about 50-ms later. The associated spectrogram from a gate depth of 50 mm corroboratively shows a decelerating embolus that appears to go near zero velocity. In Fig. 7b, the sample gate depth of the spectrogram is placed near the proximal edge of the ACA flow signal. The spectrogram reveals that there are two blood flow signals in the image—the flow toward the probe, which is a relatively weak signal, is from the internal carotid artery (ICA) or the proximal MCA, and the ACA flow away from the probe is the dominant signature. The communication between these vessels, and confirmation that the ICA is present to some degree in the spectrogram, is demonstrated by the passage of a microembolus from the ICA (red) to the ACA (blue). The initial embolic signal is directed toward the probe in the spectrogram and shows as a transient red track in the PMD image. The direction change occurs in a time window on the order of 10-ms and a much longer embolic signal (blue track in PMD image) is then observed in the ACA. When two vessels are in the sample volume, as in Fig. 7b, the mean velocity of all signals contained in the sample volume determines the color of the PMD image. Vessels presenting stronger US reflections from blood because of their position in the US beam will bias this mean.

Figure 7c shows multiple emboli apparently entering the proximal segment of the MCA, but only the last embolus traverses to a gate depth of 50 mm and is seen in the spectrogram. The others have either come to rest or exited *via* branch vessels. This demonstrates the limited sensitivity in single-gate transcranial Doppler monitoring for microemboli moving to the brain through the ICA. This point is further illustrated in the case of a 62-year-old patient undergoing coronary artery bypass surgery and aortic valve replacement. During 60 min of continuous monitoring with the TCD100M, 105 emboli were noted on the PMD display. At the same time, the spectrogram placed at the depth of 50 mm in the MCA detected only 35 (33%) of the embolic signatures seen on the PMD display. The other signals represent emboli passing through the ipsilateral or contralateral ACA and other branches of the ipsilateral proximal MCA.

Figure 8 illustrates cerebral bubble microembolic signals from IV injection of 10 mL of agitated saline. The patient had a stroke and was undergoing catheter closure of a patent foramen ovale while being monitored with PMD. The shower of microemboli illustrates the

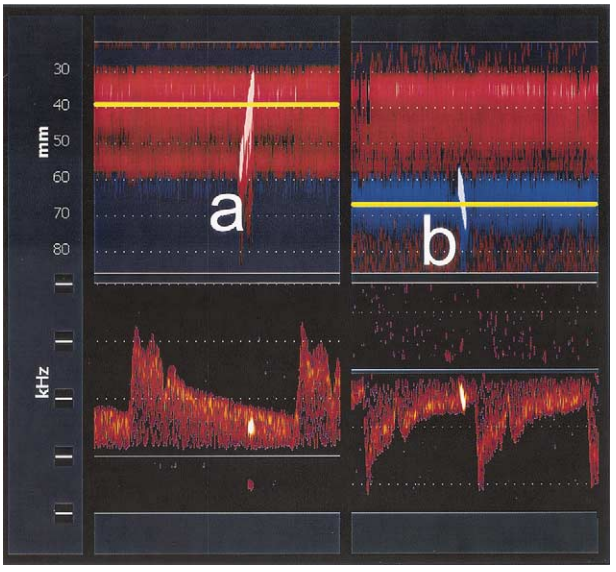

Fig. 6. (a) MCA and (b) ACA embolic signatures observed with TCD100M in subject with prosthetic heart valves.

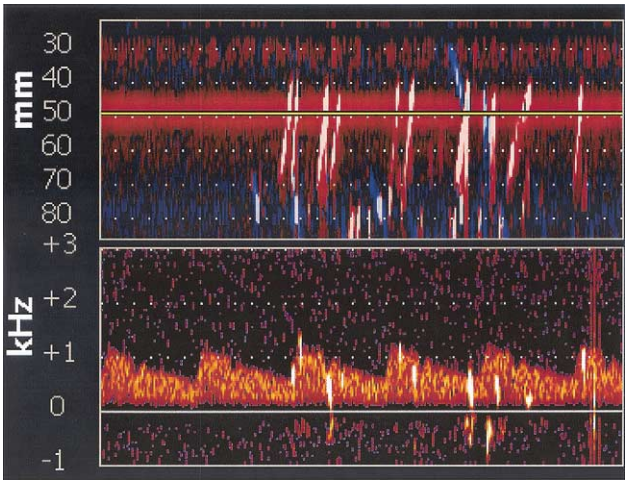

Fig. 8. Cerebral microembolic shower from IV injection of 10 mL agitated saline in acute stroke patient undergoing catheter repair of patent foramen ovale.

greater sensitivity of PMD over that of a single-gate Doppler. Although only 10 embolic signatures can be counted within the spectrogram, there are many more evident in the ipsilateral ICA and both ACAs. The greater dynamic range of the digital Doppler is evident from the absence of extraspectral aliasing, so often produced by bubble embolic signals in analogue spectral displays. An interesting delay in movement of one bubble in a branch of the MCA is disclosed by the blue embolic track at a depth of 40 mm. Strongly echoic microemboli can transit across side lobes or weakly insonated regions of the US beam that are insensitive to blood flow. The resulting signatures give the impression that the microembolus is moving in areas where either no blood is flowing or in areas where the predominant blood flow is moving in opposite direction to the microembolus. This phenomenon is demonstrated repeatedly in Fig. 8.

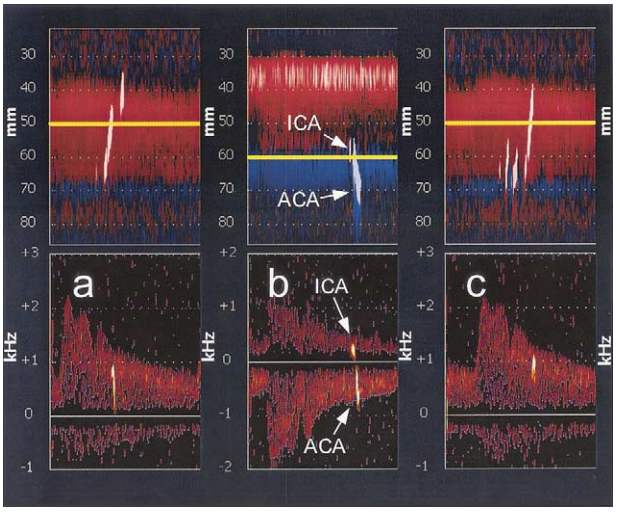

Fig. 7. Complex embolus behavior demonstrated by PMD display: (a) Embolus coming to ~50 ms rest in MCA and then continuing into distal MCA segment. (b) Embolus movement from ICA to ACA. (c) Multiple emboli, one of which traverses the MCA and the Doppler sample volume associated with the spectrogram.

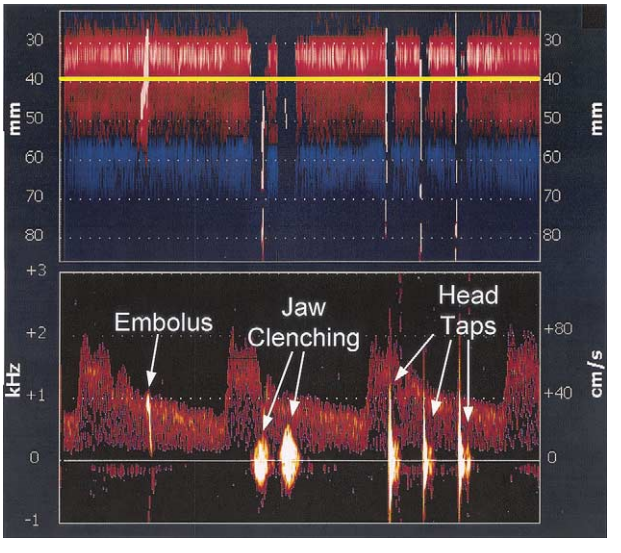

Fig. 9. Jaw-clenching and head-tap artefacts presented beside an embolic signal. These signals are high-intensity transients in the spectrogram, but behave differently in the power M-mode image: the embolus appears as a characteristic embolic track and the artefacts show as darkened regions.

PMD displays artefact signals in a fashion that is easily differentiated from embolic tracks. Figure 9 shows an embolic signal along side jaw clenching and head tapping. The spectrogram shows high-intensity bidirectional transient signals and PMD suppresses these signals from the display. The PMD image shows simultaneous interference that occurs at all depths during jaw movements or tapping on the head. This behavior is due to clutter filtering of mean velocity in the PMD display; signals that have mean velocity less than 200 Hz in this image are colored black. The initial experience with PMD has shown that all artefact signals have these two properties of 1. yielding mean velocities below the clutter cutoff and 2. doing so uniformly across depth. These properties are anticipated to be fundamental tools for automatically discriminating embolic tracks from artefacts in the PMD image. Note within the regions of black in Fig. 9 there are thin vertical high-intensity streaks. These happen in association with artefacts in brief time episodes where the average apparent velocity is greater than 7 cm/s, and are not seen to detract from the ability to use the larger surrounding blacked-out region to classify the artefactual signal type.

DISCUSSION AND SUMMARY

PMD has several advantages over traditional TCD using the single or multigate spectrogram, due to its ability to simultaneously display the power and direction of the blood flow signatures over a wide range of depth. Although this is the first exploratory report, and the clinical value of PMD requires prospective studies, the following potential clinical advantages of PMD over traditional TCD were identified:

1. Transcranial windows can be easily found and maintained.
2. It is not necessary to seek a window by changing depth or listening for a Doppler sound.
3. PMD facilitates vessel identification using depth and direction of flow.
4. Signatures of turbulence and velocity aliasing can identify arterial stenosis, notably in branching vessels, facilitating a more thorough and repeatable TCD examination.
5. Microembolic signals present a unique signature or "track" in the PMD image, which defines them as representing emboli.
6. Artefacts by contrast are suppressed from the PMD image.

Other advantages are anticipated with further clinical exploration.

Complex embolic signals such as those in Fig. 7b have been observed spectrally in prosthetic valve patients and in a pig model of human cerebral embolism (Ishii et al. 1999). The "tail sign" phenomenon in the spectrogram is an embolic signal depicting embolus movement in one direction quickly followed by an embolic signal in the opposite direction, with a prevalence of 73% in the pig model. The experience reported here with a subject having two prosthetic valves is that the complex behavior is observed to the extent that multiple vessels are seen by the US beam and, therefore, in the PMD display. Placing the beam in the vicinity of the ICA termination and the MCA/ACA takeoff, or in the distal region of the MCA where the M2 branch vessels can turn and move blood away from the temporal window, results in more observations of complex "tail-sign" behavior than if the beam is looking in skew fashion at the M1 segment of the MCA.

The PMD display presents a nonambiguous modality for automatic detection of microemboli and differentiation from artefact. A vertical slice through any region of an embolic signature on the PMD display produces a sampling of power vs. depth and has a unimodal peak, given the presence of one embolus. This intensity peak is a "fixed time" 8-ms snapshot of an embolus and has a width at half maximum amplitude proportional to the sample volume size (Moehring 2001). Pattern recognition of embolic tracks along the depth axis for each fixed time is, therefore, anticipated to be a more sensitive and specific method to automatically detect microemboli at all depths in the PMD image than monitoring one to several single-gate Doppler outputs along the time axis.

The PMD modality is more definitive than traditional TCD for detecting microemboli going to the brain *via* the internal carotid artery, by virtue of its abilities to monitor embolus traffic over a broad depth range, in the proximal MCA and ACA simultaneously, and to separate emboli unambiguously from artefacts. This has significant implication for transcranial monitoring for emboli from active lesions in the heart or neck—the yield in this activity stands to be much higher if the PMD modality is utilized. Ultimately, an embolus fundamentally declares itself on PMD or in single-gate Doppler by having sufficient embolus-to-blood power ratio (EBR) (*i.e.*, US reflections above the background blood flow also under observation) (Moehring and Klepper 1994). The PMD method puts this facet of microemboli directly in view with the associated movement along a vascular path much larger than the single-gate Doppler sample volume.

Emboli of sufficient composition and size can saturate the front end for any transcranial Doppler receiver, but the PMD modality does not suffer the same saturation phenomenon seen in the spectrogram. Signal saturation in the vicinity of an embolus will never saturate signals from scatterers that are closer to the probe than the embolus, so extraspatial artefacts will not appear

between the embolus and the probe. So, although a spectrogram may develop vertical broad-band extraspectral streaks due to strong embolic reflections, the PMD display is limited in this respect. The shallow edge of the embolic track will generally maintain a sloping well-behaved character because it represents a high-amplitude reflector moving in time and space.

We developed power M-mode Doppler (PMD) as a new modality to address the problem of difficult transcranial detection of blood flow and as a platform for automatic detection of microemboli. These goals required setting aside traditional Doppler US analog electronics in favor of digitally sampling US echoes before Doppler signal extraction. The PMD image and simultaneous spectrogram were then accomplished with software in the digital environment. Initial clinical exploration of this modality in our vascular laboratory shows promising results for each goal. Further development is underway in our laboratory for using PMD to automatically detect microemboli. Work is also underway to enhance this modality for observing blood flow pathology and to corroborate our findings in other vascular laboratories.

Acknowledgement—This work was supported in part by National Institutes of Health SBIR grant 2R44HL57108-02. The authors gratefully acknowledge the technical team—Henry Baron, Mark Curry, Troy Lehto, Grant Mattson, Marc McDaniel, Rowena Miyashiro, Tim Myers, Randy Radford, Scott Seidel, Tony Williams, Arne Voie and Brian Wilson—and the clinical team—David Amory, David Dobson, Kari May, Cees Verkerk, John White and Ajay Zachariah for the many hours and creative energy that made this work possible.

REFERENCES

Ackerstaff RGA, Babikian VL, Georgiadis D, et al. Basic identification criteria of Doppler microembolic signals. Stroke 1995;26:1123.

Ackerstaff RGA, Moons KGM, van de Vlasakker CJW, et al. Association of intraoperative transcranial Doppler monitoring variables with stroke from carotid endarterectomy. Stroke 2000;31:1817–1823.

Cullinane M, Reid G, Dittrich R, et al. Evaluation of new online automated embolic signal detection algorithm, including comparison with panel of international experts. Stroke 2000;31:1335–1341.

Eyer MK, Brandestini MA, Phillips DJ, Baker DW. Color digital echo/Doppler image presentation. Ultrasound Med Biol 1981;7:21–31.

Ishii M, Eto G, Tei C, et al. "Tail sign" associated with microembolic signals. Stroke 1999;30:863–866.

Kasai C, Namekawa K, Koyano A, Omoto R. Real-time two-dimensional blood flow imaging using an autocorrelation technique. IEEE Trans Sonics Ultrason 1985;SU-32:458–464.

Moehring MA. Microembolus tracking with power M-mode transcranial Doppler ultrasound and simultaneous single gate spectrogram (Abstr.). Cerebrovasc Dis 2000;10(Suppl. 1):2.

Moehring MA. Axial lengths of power M-mode microembolus (ME) tracks are proportional to sample volume size (Abstr.). Cerebrovasc Dis 2001;11(Suppl. 3):4.

Moehring MA, Klepper JR. Pulse Doppler ultrasound detection, characterization and size estimation of emboli in flowing blood. IEEE Trans Biomed Eng 1994;41(1):35–44.

Nabavi DG, Georgiadis D, Mumme T, Zunker P, Ringelstein EB. Detection of microembolic signals in patients with middle cerebral artery stenosis by means of a bigate probe. A pilot study. Stroke 1996;27:1347–1349.

Omoto R, Yokote Y, Takamoto S, et al. The development of real-time two-dimensional Doppler echocardiography and its clinical significance in acquired valvular diseases. Jpn Heart J 1984;25:325–340.

Padayachee TS, Parsons S, Theobold R. The detection of microemboli in the middle cerebral artery during cardiopulmonary bypass: A transcranial Doppler ultrasound investigation using membrane and bubble oxygenation. Ann Thorac Surg 1987;44:298–302.

Ringelstein EB, Droste DW, Babikian VL, et al. for the International Consensus Group on Microembolus Detection. Consensus on microembolus detection by TCD. Stroke 1998;29:725–729.

Spencer MP. Detection of cerebral arterial emboli. In: Newell DA, Aaslid R, eds. Transcranial Doppler. New York, NY: Raven Press, 1992:212–230.

Spencer MP. Transcranial Doppler monitoring and causes of stroke from carotid endarterectomy. Stroke 1997;28:685–691.

Spencer MP, Thomas GI, Nicholls SC, Sauvage, LR. Detection of middle cerebral artery emboli during carotid endarterectomy using transcranial Doppler ultrasonography. Stroke 1990;21:415–423.